The DNA Intercalating Alkaloid Cryptolepine Interferes with Topoisomerase II and Inhibits Primarily DNA Synthesis in B16 Melanoma Cells†

K. Bonjean,*,‡ M. C. De Pauw-Gillet,‡ M. P. Defresne,‡ P. Colson,§ C. Houssier,§ L. Dassonneville,|| C. Bailly,*,|| R. Greimers,⊥ C. Wright,# J. Quetin-Leclercq,¶,+ M. Tits,¶ and L. Angenot¶

Laboratoire d'Histologie et de Cytologie, Institut d'Anatomie (L3), Université de Liège, Rue de Pitteurs, 20, 4020 Liège, Belgium, Laboratoire de Chimie Macromoléculaire et Chimie Physique, Institut de Chimie, Université de Liège, Sart-Tilman (B6), 4000 Liège, Belgium, Laboratoire de Pharmacologie Antitumorale du Centre Oscar Lambret et INSERM U124, IRCL, Place de Verdun, 59045 Lille, France, Laboratoire d'Anatomie et Cytologie Pathologiques, CHU de Liège (B23), 4000 Liège, Belgium, Postgraduate Studies in Pharmaceutical Technology, The School of Pharmacy, University of Bradford, West Yorkshire BD7 4ER, U.K., and Laboratoire de Pharmacognosie and Institut de Pharmacie, Université de Liège, Rue Fusch, 5, 4000 Liège, Belgium

Received December 1, 1997; Revised Manuscript Received January 28, 1998

ABSTRACT: Cryptolepine hydrochloride is an indoloquinoline alkaloid isolated from the roots of *Cryptolepis sanguinolenta*. It is characterized by a multiplicity of host-mediated biological activities, including antibacterial, antiviral, and antimalarial properties. To date, the molecular basis for its diverse biological effects remains largely uncertain. Several lines of evidence strongly suggest that DNA might correspond to its principal cellular target. Consequently, we studied the strength and mode of binding to DNA of cryptolepine by means of absorption, fluorescence, circular, and linear dichroism, as well as by a relaxation assay using DNA topoisomerases. The results of various optical and gel electrophoresis techniques converge to reveal that the alkaloid binds tightly to DNA and behaves as a typical intercalating agent. In DNAase I footprinting experiments it was found that the drug interacts preferentially with GC-rich sequences and discriminates against homo-oligomeric runs of A and T. This study has also led to the discovery that cryptolepine is a potent topoisomerase II inhibitor and a promising antitumor agent. It stabilizes topoisomerase II−DNA covalent complexes and stimulates the cutting of DNA at a subset of preexisting topoisomerase II cleavage sites. Taking advantage of the fluorescence of the indoloquinoline chromophore, fluorescence microscopy was used to map cellular uptake of the drug. Cryptolepine easily crosses the cell membranes and accumulates selectively into the nuclei rather than in the cytoplasm of B16 melanoma cells. Quantitative analyses of DNA in cells after Feulgen reaction and image cytometry reveal that the drug blocks the cell cycle in G_2/M phases. It is also shown that the alkaloid is more potent at inhibiting DNA synthesis rather than RNA and protein synthesis. Altogether, the results provide direct evidence that DNA is the primary target of cryptolepine and suggest that this alkaloid is a valid candidate for the development of tumor active compounds.

Cryptolepine hydrochloride (Figure 1) is a yellow indoloquinoline alkaloid whose anhydronium base, formed in concentrated alkali, shows a deep-purple coloration. This natural product was first isolated from the roots of *Cryptolepis triangularis* collected in Belgian Congo (*1*, *2*, *54*) and afterward from the roots of *Cryptolepis sanguinolenta* from Nigeria (*3*). The determination of its structure was based on chemical reactions of a degradative nature and on ultraviolet spectroscopy in neutral and basic media (*3*). ^{1}H NMR and ^{13}C NMR and MS data have confirmed the proposed structure (*4*−*6*). Cryptolepine was also isolated from the Sri Lanka plant *Sida acuta* and detected in *Sida rhombifolia* (*7*).

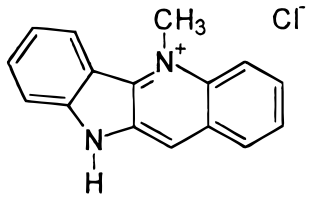

FIGURE 1: Structure of cryptolepine [5-methylquinolo-(2′,3′,3,2)-indole].

Extracts from *Cryptolepis* plants have been used in African folk medicine as a remedy against colic, as a stomach tonic, as well as in the treatment of infectious diseases, including malaria. The main alkaloid cryptolepine has been reported

† This work was supported by research grants from the Ligue Nationale Française Contre le Cancer (Comité du Pas-de-Calais) and the Fédération Nationale des GEFLUC (to C.B.) and from the Actions de Recherches Concertées Grant 95/00-93 (to C.H. and P.C.). Support from the "convention INSERM-CFB" is acknowledged, and from Fonds Spéciaux pour la Recherche dans les Universités (to L.A. and M.P.D.).

* Authors to whom correspondence should be addressed.
‡ Institut d'Anatomie, Université de Liège.
§ Institut de Chimie, Université de Liège.
|| COL-INSERM.
⊥ CHU de Liège.
University of Bradford.
¶ Institut de Pharmacie, Université de Liège.
+ Present address: Laboratoire de Pharmacognosie, CHAM 7230, Université Catholique de Louvain, Av. E. Mounier, 72, 1200 Bruxelles, Belgium.

S0006-2960(97)02927-9 CCC: $15.00
Published on Web 03/19/1998

to produce a variety of pharmacological effects; these include hypotensive and antipyretic properties (*8*−*10*), presynaptic α-adrenoreceptor blocking action (*11*), antimuscarinic properties (*12*), anti-inflammatory properties (*13*), antibacterial effects (*14*−*17*), and antimalarial activity (*18*−*21*).

However, relatively little is known concerning the mechanism of action of cryptolepine. Indeed, there is some justification to believe that cryptolepine exerts its biological activity via an interaction with DNA. On one hand, cryptolepine shows structural similarities with ellipticine, which is a well-known DNA intercalating agent (*22*). Hydroxylated derivatives of ellipticine interfere with topoisomerase II (*23*) and display a useful spectrum of antitumor activity *in vivo* (*24*−*25*), thus raising the intriguing possibility that cryptolepine too might affect topoisomerase II functions and be selectively toxic for cancer cells. On the other hand, a recent study suggested that cryptolepine interacts with DNA, as judged from preliminary absorption measurements (*18*). In addition, we have reported that cryptolepine competes with the triphenylmethane dye methyl green for binding to DNA with the same efficiency as the well-known intercalating drug doxorubicin (*26*). That cryptolepine displays antiparasitic activity may also be considered as an indication of propensity to bind to DNA, since numerous antiviral and antimalarial drugs interact with DNA and/or inhibit topoisomerase II (*27*, *28*). Nevertheless, despite the evidence accumulated to date indicating that direct interaction with the genome of the pathogen may contribute to the pharmacological effect of cryptolepine, the binding of this alkaloid to DNA has never been thoroughly investigated, and as a consequence our knowledge as to the molecular mechanism of action of this drug remains very sparse.

These observations prompted us to examine the issue of DNA binding and topoisomerase II poisoning by cryptolepine. The present investigation began with an attempt to delineate the strength and the mode of binding of cryptolepine to DNA. Absorption measurements as well as circular and electric linear dichroism experiments were performed with the alkaloid, reinforced by fluorescence emission and thermal denaturation studies. Topological methods were applied to assay the relative ability of the drug to unwind supercoiled DNA. The sequence specificity of binding was determined by DNAase I footprinting experiments on several DNA restriction fragments of defined sequence. In addition, we investigated the effect of the drug on topoisomerase II−DNA cleavable complex formation. We measured the cytotoxicity of the drug toward mouse B16 melanoma cells and studied its effects on the synthesis of DNA, RNA, and protein. Finally, a quantitative DNA content study was performed, providing thus a more complete description of the pharmacological profile of cryptolepine.

MATERIALS AND METHODS

Drug. Cryptolepine hydrochloride was isolated and purified from *C. sanguinolenta* as described elsewhere (*20*). It was dissolved in methanol at 10^{-2} M concentration for physicochemical experiments and in water at 4×10^{-4} M for the cell culture studies. Drug concentrations were determined spectrophotometrically using an absorption coefficient of 28 600 M^{-1} cm^{-1} at 369 nm in methanol.

Chemicals and Biochemicals. Calf thymus DNA and the double-stranded polymers poly(dA-dT)·poly(dA-dT), poly(dI-dC)·poly(dI-dC), poly(dA-dC)·poly(dG-dT), and poly(dG-dC)·poly(dG-dC) were from Pharmacia (Uppsala, Sweden). Their concentrations were determined applying molar extinction coefficients of 6600, 6600, 6900, 7000, and 8400 M^{-1} cm^{-1}, respectively (*29*). Calf thymus DNA was deproteinized with sodium dodecyl sulfate (protein content <0.2%), and all nucleic acids were dialyzed against 1 mM sodium cacodylate buffered solution (pH 6.5). Nucleoside triphosphates labeled with ^{32}P (α-dATP and γ-ATP) were obtained from Amersham (Buckinghamshire, England) (3000 Ci/mmol). Restriction endonucleases *Ava*I, *Eco*RI, *Hin*dIII, and *Pvu*II, alkaline phosphatase, T4 polynucleotide kinase, and AMV reverse transcriptase were purchased from Boehringer (Mannheim, Germany) and used according to the supplier's recommended instructions in the activity buffer provided.

Absorption Spectroscopy. Absorption spectra were recorded on a Perkin-Elmer Lambda 5 spectrophotometer using a 10 mm optical path length. Titrations of the drug with DNA, covering a large range of DNA phosphate/drug ratios (*P*/*D*), were performed by adding aliquots of a concentrated DNA solution to a drug solution at constant ligand concentration (20 μM). DNA blanks at the same nucleotide concentrations were prepared concomitantly and used as a reference in the recording of absorption spectra. Binding constants were determined using experimental spectrophotometric readings from absorbance titration experiments conducted at 367 nm. The apparent association constants K (M^{-1}) and number of sites per nucleotide were estimated from Scatchard plots.

The circular dichroism (CD) spectra were recorded on a Jobin-Yvon CD 6 dichrograph interfaced to a microcomputer. Solutions of drugs, nucleic acids, and their complexes in 1 mM sodium cacodylate buffer (pH 6.5) were scanned in 1 cm quartz cuvettes. Measurements were made by progressive dilution of drug−DNA complexes at a high *P*/*D* (phosphate/drug) ratio with a pure ligand solution to yield the desired drug/DNA ratio. Three scans were accumulated and automatically averaged. Results are expressed in molar circular dichroism $\Delta\epsilon = \Delta A/lc$ where ΔA is the circular dichroism amplitude, l is the cell path length, and c is the total ligand concentration.

Electric linear dichroism (ELD) measurements were performed with a computerized optical measurement system (*30*, *31*) using the procedures previously outlined (*32*). All experiments were conducted with a 10 mm path length Kerr cell having 1.5 mm electrode separation. The samples were oriented under an electric field strength varying from 1 to 13 kV/cm. The drug under test was present at a concentration of 10 μM together with the DNA at 100 μM unless otherwise stated. This electro-optical method has proved most useful as a means of determining the orientation of the drugs bound to DNA and has the additional advantage that it senses only the orientation of the polymer-bound ligand; free ligand is isotropic and does not contribute to the signal (*33*, *34*).

Fluorescence measurements were carried out on a Perkin-Elmer LS 50 Spectrofluorimeter. Fluorescence emission spectra were measured from 480 to 620 nm with an excitation wavelength of 426 nm.

Melting Temperature Studies. Melting curves were measured using an Uvikon 943 spectrophotometer coupled to a Neslab RTE111 cryostat. For each series of measurements, 12 samples were placed in a thermostatically controlled cell-holder, and the quartz cuvettes (10 mm path length) were heated by circulating water. The measurements were performed in BPE buffer (pH 7.1) (6 mM Na_2HPO_4, 2 mM NaH_2PO_4, 1 mM EDTA). The temperature inside the cuvette was measured with a platinum probe; it was increased over the range 20−100 °C with a heating rate of 1 °C/min. The melting temperature T_m was taken as the midpoint of the hyperchromic transition.

DNA Purification and Labeling. Plasmids pBS (Stratagene, La Jolla, CA) and pLAZ3 (*35*) were isolated from *Escherichia coli* by a standard sodium dodecyl sulfate−sodium hydroxide lysis procedure and purified by banding in CsCl−ethidium bromide gradients. Ethidium was removed by several 2-propanol extractions followed by exhaustive dialysis against Tris−EDTA buffered solution. The purified plasmid was then precipitated and resuspended in appropriate buffered medium prior to digestion by the restriction enzymes. The two pBS DNA fragments were prepared by 3′-^{32}P-end labeling of the *Eco*RI−*Pvu*II double digest of the plasmid using [α-^{32}P]dATP and AMV reverse transcriptase or by 5′-^{32}P-end labeling of the *Eco*RI/alkaline phosphatase treated plasmid using [γ-^{32}P]ATP and T4 polynucleotide kinase followed by treatment with *Pvu*II. Similarly, the 155-mer and 178-mer fragments were prepared by 3′-end labeling of the *Eco*RI−*Hin*dIII and *Eco*RI−*Pvu*II digests, respectively, of plasmid pLAZ3. In each case, the digestion products were separated on a 6% polyacrylamide gel under native conditions in TBE buffered solution [89 mM Tris-borate (pH 8.3), 1 mM EDTA]. After autoradiography, the band of DNA was excised, crushed, and soaked in water overnight at 37 °C. This suspension was filtered through a Millipore 0.22 μm filter, and the DNA was precipitated with ethanol. Following washing with 70% ethanol and vacuum-drying of the precipitate, the labeled DNA was resuspended in 10 mM Tris adjusted to pH 7.0 containing 10 mM NaCl.

DNA Unwinding Experiments. Supercoiled pBS DNA (0.5 μg) was incubated with 6 units of topoisomerase I or topoisomerase II (TopoGen Inc., Columbus, OH) at 37 °C for 1 h in relaxation buffer [50 mM Tris (pH 7.8), 50 mM KCl, 10 mM $MgCl_2$, 1 mM dithiothreitol, 1 mM EDTA] in the presence of varying concentrations of cryptolepine. Reactions were terminated by extraction with neutralized phenol. DNA samples were then added to the electrophoresis dye mixture (3 μL) and electrophoresed (35 V/cm) in a 1% agarose gel at room temperature for 15 h. Gels were stained with ethidium bromide (1 mg/mL), washed, and photographed under UV light.

Topoisomerase II DNA Cleavage Reaction. The cleavage reaction mixture contained 20 mM Tris-HCl (pH 7.4), 60 mM KCl, 0.5 mM EDTA, 0.5 mM dithiothreitol, 10 mM $MgCl_2$, 1 mM ATP, 500 cps of [γ-^{32}P]pBS DNA, and the indicated drug concentrations. The reaction was initiated by the addition of human topoisomerase II (20 units in 20 μL reaction volume, p170 form from TopoGen Inc.) and allowed to proceed for 30 min at 37 °C. Reactions were stopped by adding SDS to a final concentration of 0.25% and proteinase K to 250 μg/mL, followed by incubation for 30 min at 50 °C. Five milliliters of loading buffer [30 mM EDTA, 15% (w/v) sucrose, 0.1% electrophoresis dye] were added to each sample prior to loading onto a 1% agarose gel in TBE buffered solution containing 0.1% SDS. Electrophoresis was conducted at 2 V/cm for 18 h.

DNAase I footprinting experiments were performed essentially as previously described (*36*). Briefly, reactions were conducted in a total volume of 10 μL. Samples (3 μL) of the labeled DNA fragments were incubated with 5 μL of the buffered solution containing the ligand at appropriate concentration. After 30 min incubation at 37 °C to ensure equilibration of the binding reaction, the digestion was initiated by the addition of 2 μL of a DNAase I solution whose concentration was adjusted to yield a final enzyme concentration of about 0.01 unit/mL in the reaction mixture. After 3 min, the reaction was stopped by freeze-drying. Samples were lyophilized and resuspended in 5 μL of an 80% formamide solution containing tracking dyes. The DNA samples were then heated at 90 °C for 4 min and chilled in ice for 4 min prior to electrophoresis.

Electrophoresis and Quantitation by Storage Phosphor Imaging. DNA cleavage products were resolved by polyacrylamide gel electrophoresis under denaturating conditions (0.3 mm thick, 8% acrylamide containing 8 M urea). After electrophoresis (about 2.5 h at 60 W, 1600 V in TBE buffered solution, BRL sequencer model S2), gels were soaked in 10% acetic acid for 10 min, transferred to Whatman 3MM paper, and dried under vacuum at 80 °C. A Molecular Dynamics 425E PhosphorImager was used to collect data from the storage screens exposed to dried gels overnight at room temperature. Baseline-corrected scans were analyzed by integrating all the densities between two selected boundaries using ImageQuant version 3.3 software. Each resolved band was assigned to a particular bond within the DNA fragments by comparison of its position relative to sequencing standards generated by treatment of the DNA with dimethyl sulfate (G) and/or formic acid (G+A) followed by piperidine-induced cleavage at the modified bases in DNA.

Cell Lines. B16 melanoma cells were obtained from subcutaneous primitive tumors implanted into a C57 Black 6J mouse. Isolated cells were first cultured as monolayers in T75 flasks containing 25 mL Minimum Eagle's Medium (MEM-GIBCO) supplemented with 10% fetal bovine serum (GIBCO) and 100 U/mL penicillin, in a humidified atmosphere (5% CO_2) at 37 °C. After reaching confluence, the cells were exposed to 0.1% trypsin−0.02% EDTA for 5 min; "fresh" cells were diluted five times for further culture in the same medium.

Cell Survival Assay. The cytotoxicity of cryptolepine toward B16 melanoma cells was assessed using the MTT test (*37*). In each well of a 96-well microtitration plate, 200 μL of medium containing 5000 cells was inoculated. Twenty four hours later, the medium was removed and replaced with 200 μL/well of fresh medium containing 0.05−1 μg/mL (0.22−4.4 μM) cryptolepine. Six wells minimum were used for each condition. After 72 h of treatment, the MTT [3-(4,5-dimethylthiazol-2-yl)-2,5-diphenyltetrazolium bromide] test was applied (*37*). The culture medium was then removed, and 100 μL of DMSO was added at room temperature and thoroughly mixed to dissolve the dark blue crystals. After a few minutes, plates were analyzed on a Labsystems Multiskan MS (type 352) reader at 570 and 620 nm.

Fluorescence Microscopy. About 5000 cells were cultured on coverslips (20 mm × 20 mm) in a Petri dish with 2 mL MEM-FBS. After 24 h, the cells were treated with 5 μg/mL (22 μM) cryptolepine and immediately analyzed on the fluorescence microscope with an excitation filter at 420 nm and an emission filter at 520 nm.

([3]H)Thymidine, ([3]H)Leucine, or ([3]H)Uridine Uptake. Fifty thousand cells were seeded into each well of a NUNC 96-well microtitration plate with 150 μL MEM-FBS containing 3 μCi/mL (^{3}H)thymidine (TdR) (1 mCi/mL, 5 Ci/mM, Amersham), 13 μCi/mL (^{3}H)leucine (Leu) (1 mCi/mL, 45−85 Ci/mM, Amersham), 7 μCi/mL (^{3}H)uridine (UdR) (1 mCi/mL, 25−30 Ci/mM, Amersham), and 0.5−3.5 μg/mL (2.2−15.5 μM) cryptolepine. The plates were incubated for 4 h at 37 °C in an air−CO_2 5% incubator. The cells were then collected on a filter (Skatron-11731) with a semi-automated cell harvester (Skatron-7019). After the first filtration, the attached cells were trypsinated and then collected on a second filter (by another aspiration). Dried filters were placed in vials, each containing two filters corresponding to the same well and 2 mL of scintillating liquid [Ready Safe Cocktail (Beckman)]. The radioactivity was then counted with a Multipurpose Scintillation Counter (Beckman LS 6500). At least eight wells were used for each drug concentration.

Quantitative analysis of DNA after Feulgen reaction was performed by image cytometry. Two hundred fifty thousand cells were cultured on coverslips (20 mm × 20 mm) in Petri dishes with 2 mL MEM-FBS and different concentrations of the drug (0.45−4.5 μM). After 20, 48, or 72 h, the cells on coverslips were fixed 30 min in 10% neutral buffered formalin solution, rinsed in running distilled water for 5 min, and air-dried for storage until staining. Samples were hydrolyzed in 5 N HCl for 60 min at room temperature prior to Feulgen staining using the Cell Analysis Systems (CAS) purified blue stain and rinse reagents (cat. no. 54100140, Becton Dickinson). The nuclear DNA content was determined using the CAS Model 200 Image Analysis System (Becton Dickinson), equipped with the Quantitative DNA Analysis (QDA) software module, which has been previously described (*38*). The system is calibrated for mass measurements in picograms of DNA per cell using the predeposited control cells containing a known amount of DNA on a slide (cat. no. 54100120). The measured DNA index is computed by reference to the known value of DNA content in picograms (*39*) and assumption of a DNA content of 7.18 pg in human diploid cells. A minimum of 250 nuclei were counted for each drug concentration tested.

Statistical Analysis. The results of the cellular assays (MTT test−radioactivity−CAS) are expressed as means ± standard errors or as percentages (controls taken as 100%). The statistical analysis with the nonparametric Mann−Withney test was performed (*P* values lower than 0.05 were considered as significant).

RESULTS AND DISCUSSION

Absorption Spectroscopy and Fluorescence. Cryptolepine alone exhibits in the near-UV region an absorption band centered at 367 nm. Binding of the drug to DNA induces well-defined bathochromic and hypochromic effects. At high *P*/*D* (DNA phosphate/drug) values, a red-shift of 12 nm and 50% hypochromicity are observed. During titration with DNA isosbestic points at 374 and 402 nm are present, pointing to the existence of a single binding mode, even under the low ionic strength conditions used (Figure 2A).

Cryptolepine alone is a natural fluorescent compound. The fluorescence excitation spectrum has a profile similar to the absorption spectrum. Fluorescence emission spectra were measured with an excitation wavelength of 426 nm. The binding of the drug to DNA is characterized by a regular decrease of the fluorescence intensity at 530 nm until a *P*/*D* ratio of 30 is reached (data not shown).

Both of these experiments were used to determine apparent association constant(s) of the ligand to DNA and the number of sites per nucleotide *n*.

Even though the absorption spectra showed nice isosbestic points, the McGhee−von Hippel model for noncooperative binding of a ligand covering *N* sites (where *N* is the ligand site size, i.e., the reverse of *n* value) could not provide satisfactory adjustment of the two parameters ($K = 7 \times 10^5$ M^{-1} and $N = 2.5$) to fit either the absorption data at 367 nm or the fluorescence emission data at 530 nm (Figure 2B,C). Therefore, we used a two-site model (*40*), assuming the existence of two independent noncooperative types of binding, to adjust the experimental data (absorption as well as fluorescence). Values of the association constants ($K_1 = 3 \times 10^6$ M^{-1} and $K_2 = 4 \times 10^4$ M^{-1}) and of the number of ligand binding sites per nucleotide ($n_1 = 0.2$ and $n_2 = 0.5$) were obtained (Figure 2B,C). Consideration of parts B and C of Figure 2 shows the much better fit obtained with the two-site model. These values are consistent with those determined for other well-known intercalating agents such as ellipticines (*22*, *23*) and acridines (*41*).

Circular Dichroism (CD). Cryptolepine does not exhibit any intrinsic optical activity but becomes optically active when it binds to DNA. As shown in Figure 3, the CD spectra of cryptolepine−DNA complexes measured in the near-UV absorption band of the ligand exhibit a maximum (positive CD) at 382.5 nm and a minimum (negative CD) at 358 nm. The intensity of the induced CD signal depends on the *P*/*D* ratio. The molar circular dichroism $\Delta\epsilon$ rapidly increases until a *P*/*D* value of 2.5 is reached, and then it gradually decreases at higher ratios (inset in Figure 3). The fall of the CD peak at high *P*/*D* ratios is attributable to a decrease of excitonic coupling arising from the distance increase between adjacent molecules. Such biphasic evolution of the CD signal of the cryptolepine with increasing *P*/*D* ratios is characteristic of an excitonic coupling and fully consistent with an intercalative mode of binding to DNA. A similar variation of molar dichroism with the *P*/*D* ratio has been reported with other intercalating agents such as ethidium bromide (*42*), acridine orange (*43*), and ellipticine derivatives (*44*, *45*). The low value of the maximum $\Delta\epsilon$ ($\Delta\epsilon^{max} = 7$) also favors the intercalation mode (*46*).

Electric Linear Dichroism (ELD). In these experiments, DNA is oriented in an electric field, and the dichroism in the region of the absorption band of the ligand bound to DNA is probed using linearly polarized light. The intensity of the ELD signal measured in the absorption band of the ligand is dependent on the orientation of the drug transition moment relative to the direction of the DNA double helical axis.

The ELD spectrum is shown in Figure 4. Cryptolepine bound to DNA exhibits a negative reduced dichroism ($\Delta A/A \approx -0.5$ in the 340−360 nm region), indicating that the

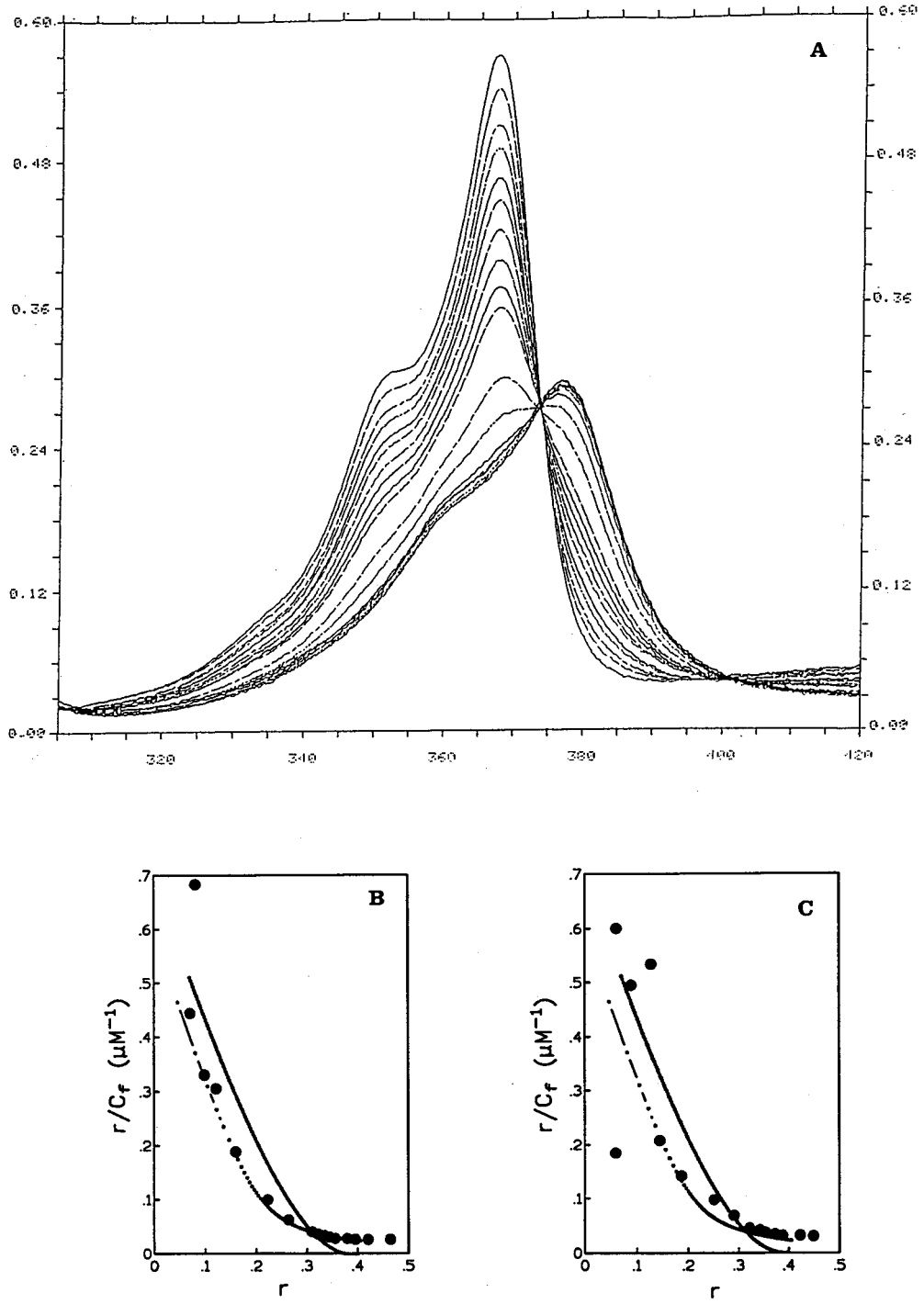

FIGURE 2: (A) Calf thymus DNA (CT-DNA) titrations of cryptolepine under low ionic strength conditions. The figure contains the absorption spectrum of the free drug (20 μM), intermediate spectra, and final spectra of the drug−DNA complexes in which the ligands have been sequestered completely by the DNA. To 3 mL of drug solution (20 μM in 1 mM sodium cacodylate buffer, pH 6.5) were added aliquots of a concentrated CT-DNA solution. Spectra are referenced against DNA solutions of exactly the same DNA concentration and were adjusted to a common baseline at 500 nm. The phosphate-DNA/drug ratio increased as follows (top to bottom curves, at 367 nm): 0, 0.2, 0.4, 0.6, 0.8, 1, 1.25, 1.5, 1.75, 2, 3, 4, 6, 8, 10, 12, 14, 16, 20. (B) Fitting of absorption data at 367 nm by the McGhee−von Hippel (full line) and the two-site model (dashed−dotted line). (C) Same as (B) for fluorescence emission data at 530 nm.

quinoloindole chromophore is oriented parallel to the DNA base pairs, a configuration consistent with an intercalative binding mode; the binding induces a stiffening effect, explaining the higher reduced dichroism value measured in the absorption band of the drug than in the free DNA absorption band ($\Delta A/A \approx -0.35$).

Thermal Denaturation. The ability of cryptolepine to alter the thermal denaturation profile of DNA is used as another indication of its propensity to bind to DNA. We measured the change of the absorbance at 260 nm as a function of the temperature for a series of DNA and polynucleotides of different base compositions in the absence and in the presence of cryptolepine. In all cases, monophasic melting curves were observed (the transition remains sharp even though the T_m changes). The variation of the T_m (ΔT_m) of helix-to-coil transition of calf thymus DNA and of the

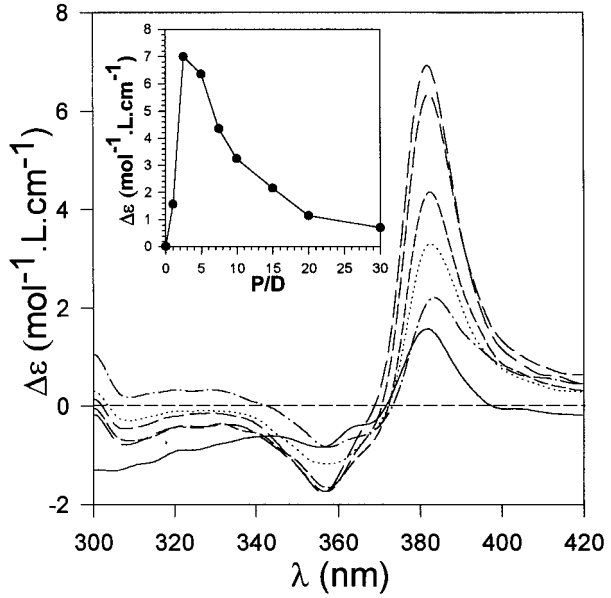

FIGURE 3: Circular dichroism spectra of the titration of cryptolepine with CT-DNA. The DNA phosphate/drug ratios (*P*/*D*) from top to bottom curves at 382.5 nm are the following: 2.5, 5, 7.5, 10, 15, 1. Inset shows the variations in molar circular dichroism $\Delta\epsilon$ (ΔA over drug concentration for 1 cm cell path length) recorded at 382.5 nm with increasing DNA/drug ratio (*P*/*D*) for cryptolepine bound to CT-DNA.

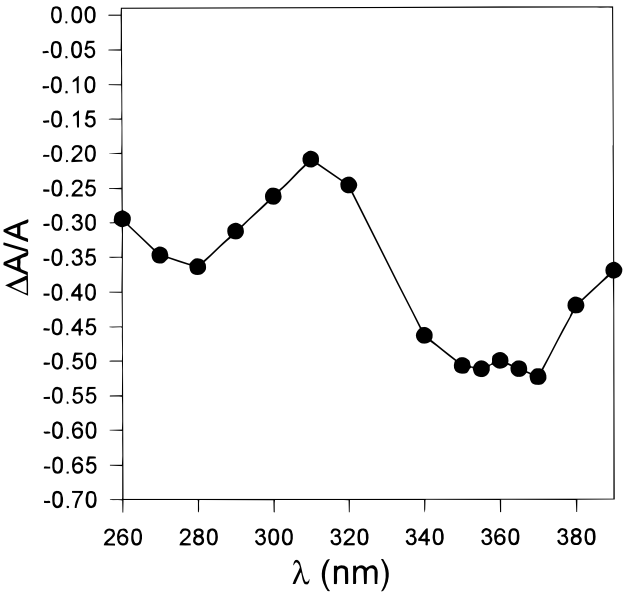

FIGURE 4: ELD spectrum of cryptolepine−DNA complexes. The reduced dichroism $\Delta A/A$ was measured at a *P*/*D* ratio of 10 under an electric field strength of 12.5 kV. Drug and CT-DNA phosphate concentrations are 10 and 100 μM, respectively.

polynucleotides (20 μM each) was determined in the presence of cryptolepine at concentrations ranging from 2 to 20 μM. The ΔT_m values are collected in Table 1.

It was not possible to study the effects on poly(dG-dC)·(dG-dC) due to its high stability, even at very low ionic strength. A large increase in the T_m value of nucleic acids is observed for the drug bound to calf thymus DNA (CT-DNA) or polynucleotides. The stabilization of the DNA double helix by binding of the drug increases with increasing molar ratio of drug to DNA phosphate (*D*/*P*). This stabilizing action of cryptolepine is very similar to that previously observed with ellipticine derivatives (*47*). Cryptolepine

Table 1: Variation in Melting Temperature (ΔT_m) on Drug Concentration and Polynucleotide Sequence[a]

	ΔT_m (°C				T_m for DNA or polynucleotide alone
	2 μM[b] 0.1[c]	5 μM[b] 0.2[c]	10 μM[b] 0.5[c]	20 μM[b] 1[c]	
poly(dA-dT)·(dA-dT)	11.6	17.4	22.7	27.8	41.1
poly(dI-dC)·(dI-dC)	9.5	15.8	19.8	26.4	34.7
poly(dA-dC)·(dG-dT)	8.8	13.7	18.6	23.2	66.7
calf thymus DNA	6.0	10.7	25.5	20.4	65.6

[a] T_m measurements were performed in BPE buffer, pH 7.1, (6 mM Na_2HPO_4, 2 mM NaH_2PO_4, 1 mM EDTA) using 20 μM DNA or polynucleotide (nucleotide concentration) in 3 mL quartz cuvettes at 260 nm with a heating rate of 1 °C/min. Each drug concentration was tested in duplicate. [b] Drug concentration. [c] Drug/DNA ratio.

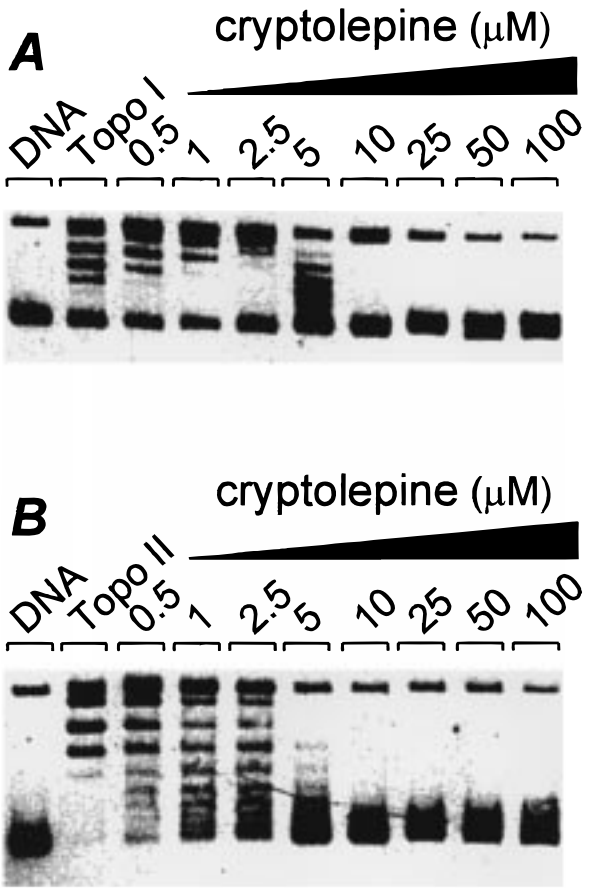

FIGURE 5: Inhibition of topoisomerase-mediated DNA supercoiling in the presence of cryptolepine. (A) Topoisomerase I and (B) topoisomerase II. Native supercoiled pAT DNA (0.5 μg) (lane DNA) was incubated for 30 min at 37 °C with 6 units of topoisomerase in the absence (lane Topo) or in the presence of a drug at the indicated concentration (μM). Reaction was stopped with sodium dodecyl sulfate and treatment with proteinase K. The DNA was analyzed by native agarose gel electrophoresis. The gels were stained with ethidium bromide and photographed under UV light.

exerts a lower stabilizing effect on CT-DNA than on the polynucleotides. The stabilization ranks in the order poly(dI-dC)·(dI-dC) > poly(dA-dT)·(dA-dT) > poly(dA-dC)·(dG-dT) > CT DNA.

Effects on Topoisomerases. Inhibition of Catalytic Activity. Closed circular DNA was treated with either topoisomerase I (Figure 5A) or topoisomerase II (Figure 5B) in the absence and in the presence of increasing concentrations

of cryptolepine. This topoisomerization assay provides a direct means to determine whether the drug affects the unwinding of closed circular duplex DNA. In both cases supercoiled DNA was relaxed by the two enzymes in the absence of the drug (lanes marked Topo I and Topo II). In the presence of cryptolepine, the relaxation reaction was totally inhibited for concentration >10 μM. The inhibition could result either from direct interference with the enzyme (e.g., stabilization of topoisomerase−DNA cleavable complexes) or from the intercalation of the drug into DNA, which also prevents the relaxation of the plasmid by the enzyme. In the topoisomerase I experiments (Figure 5A) it could be seen that at low concentrations (0.5−2.5 μM) the drug enhanced the unwinding of DNA so as to reduce the electrophoretic mobility of the topoisomers, and then at higher concentration (5 μM) the relaxation was inhibited. The effect is typical of an intercalating agent. With topoisomerase II (Figure 5B), the relaxation of DNA was inhibited even at a concentration as low as 0.5 μM, and the extent of inhibition was directly proportional to the drug concentration.

Topoisomerase-Mediated DNA Cleavage. To determine whether cryptolepine can stabilize topoisomerase−DNA cleavable complexes, we studied the effect of the drug on both purified calf thymus and human topoisomerases I or II using the ^{32}P-labeled *Eco*RI−*Pvu*II restriction fragment of pBS as a substrate. The method permits the distinction between topoisomerase inhibition and topoisomerase poisoning. The former prevents the enzyme from working (presumably by the drug binding to DNA and preventing enzyme binding) and is seen with most intercalators at a high enough concentration. The latter (enhancement of cleavage due to inhibition of religation/stabilization of cleavable complex) is seen with only a small proportion of intercalators. The DNA cleavage products were analyzed by alkaline (for topoisomerase I) or neutral (for topoisomerase II) agarose gel electrophoresis. Cryptolepine had absolutely no effect on topoisomerase I (data not shown), but it proves to inhibit topoisomerase II. The patterns of double-strand cleavage are shown in Figure 6. The effect observed with cryptolepine is similar to that obtained with the antitumor drug amsacrine which is a well-established topoisomerase II inhibitor (*48*). The cleavage appears to be stimulated at a few identical sites with amsacrine and cryptolepine (arrows in Figure 6). As observed by others with amsacrine and related anilinoacridine derivatives (*49*, *50*), there is no qualitative redistribution of the cleavage regions in DNA. Despite their structural differences, these two drugs apparently modulate the catalytic activity of the enzyme more or less similarly. At concentrations ranging from 2 to 15 μM cryptolepine stimulates DNA cleavage, but at higher concentrations (20−100 μM) the drug inhibits the cleavage of DNA by the enzyme. Inhibition of cutting at high concentrations is a common feature of DNA intercalating drugs (*51*, *52*).

Sequence Selective Binding. Footprinting studies were performed using the endonuclease DNAase I which is a very sensitive enzyme for mapping the DNA binding sites of small molecules (*36*). Four different DNA restriction fragments, isolated from the plasmids pLAZ3 and pBS and 3′- or 5′-end labeled on one or the other of the complementary strands, were used as substrates. A typical autoradiograph of a sequencing gel used to fractionate the products of partial

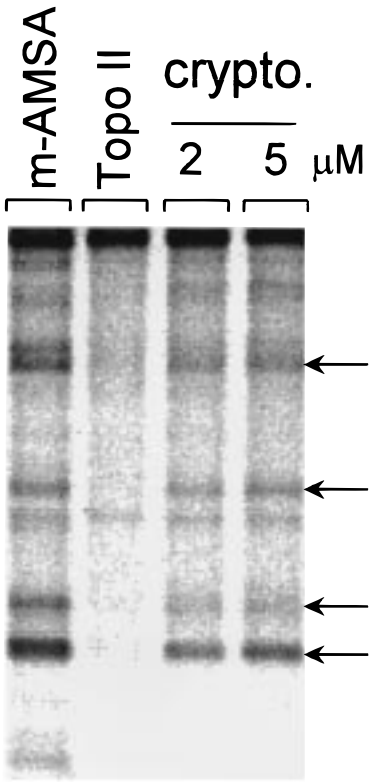

FIGURE 6: Topoisomerase II-mediated cleavage of DNA in the presence of cryptolepine (2 and 5 μM) and amsacrine (25 μM). Purified human p170 topoisomerase II (20 units) was incubated with the *Eco*RI−*Pvu*II restriction fragment from pBS (5′-end ^{32}P-labeled at the *Eco*RI site) in the absence (lane Topo II) and the presence of the test ligands. Double-stranded DNA fragments were analyzed on a 1% neutral agarose gel in the TBE buffer. Arrowheads point to the principal sites of topoisomerase II cleavage stimulated by cryptolepine.

digestion of the DNA complexed with cryptolepine is presented in Figure 7. In most cases there was no complete inhibition of DNAase I cutting (so as to produce a "gap" in the gel), but it is obvious that with the drug bound to DNA the DNAase I cleavage pattern differed significantly from that seen in the control lane. Numerous bands in the drug-containing lanes were weaker than the same bands in the drug-free lane, corresponding to attenuated cleavage, while others display relative enhancement of cutting. Many other gels (not shown) using different concentrations of cryptolepine were run and used for the quantification.

Intensities from selected gel lanes were quantified by densitometry and converted into a set of differential cleavage plots (not shown) that indicate the extent to which cleavage at each internucleotide bond is affected by complexation with cryptolepine. A summary map of the binding sites and regions of enhanced cleavage is given in Figure 8. Areas of enhanced cleavage were visible around positions 44 and 65 of the 117-mer fragments as well as at many other positions on each DNA fragment. In every case, these regions corresponded to runs of A and/or T which were poorly cut in the absence of drug, but which became much more susceptible to the cleavage in the presence of cryptolepine. Like most intercalating drugs, cryptolepine strongly discriminates between runs of adenines or thymines. In contrast, the regions of attenuated cleavage always coincide with sequences containing G·C base pairs. The two sequences 5′-GGGTAACGCCAG and 5′-CCGCGGTGGCG-

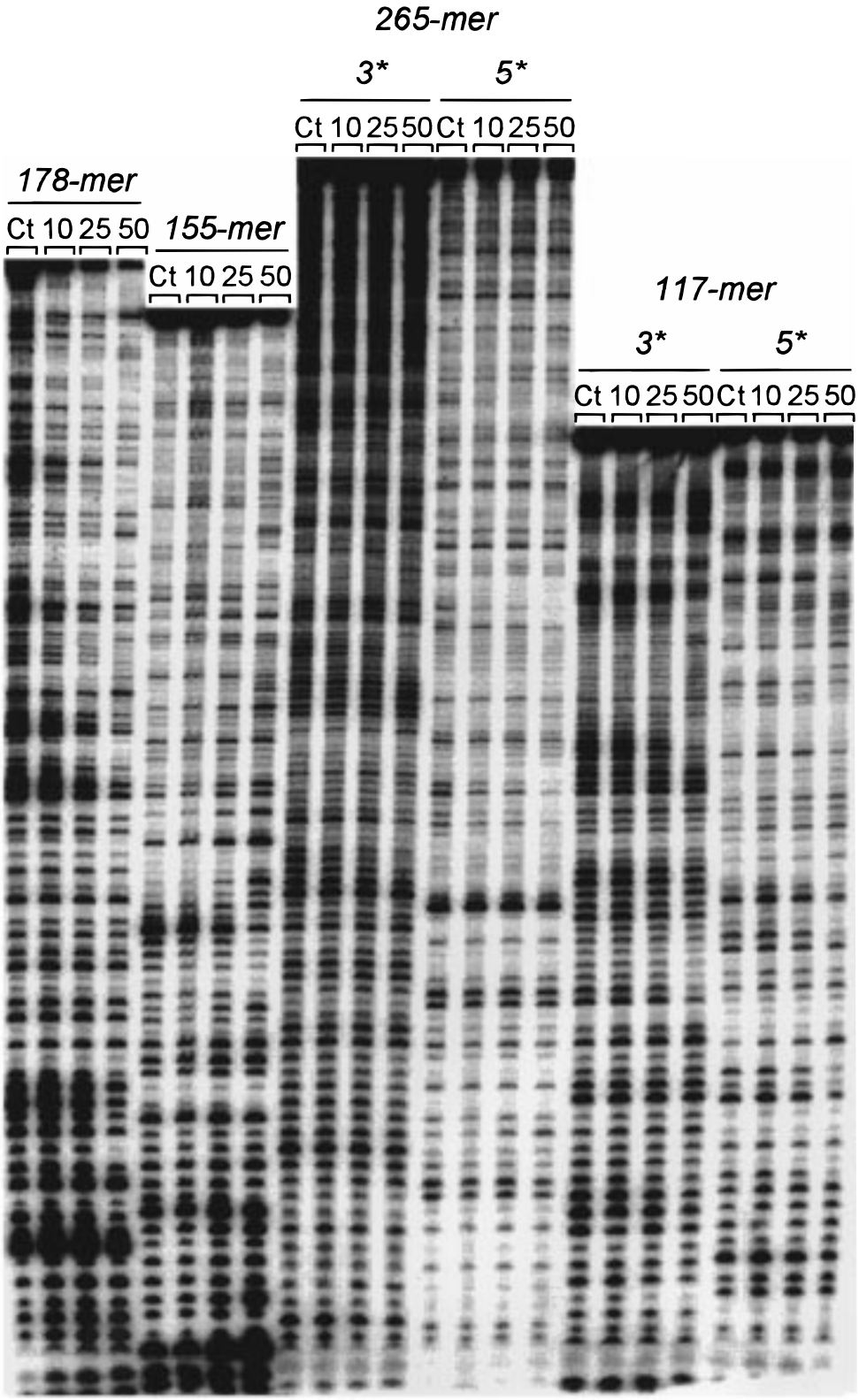

FIGURE 7: Sequence selective binding. The gels show DNAase I footprinting with the 3′-end labeled (3*) and 5′-end labeled (5*) 117-mer and 265-mer *Pvu*II−*Eco*RI restriction fragments cut from the plasmid pBS and with the 3′-end labeled 155-mer *Eco*RI−*Hin*dIII fragment and 178-mer *Eco*RI−*Pvu*II fragment from plasmid pLAZ3 in the presence of cryptolepine at 10, 25, and 50 μM concentrations. In each case, the DNA was labeled at the *Eco*RI site with either [γ-^{32}P]ATP in the presence of T4 polynucleotide kinase (5*) or [α-^{32}P]dATP in the presence of AMV reverse transcriptase. The products of nuclease digestion were resolved on an 8% polyacrylamide gel containing urea (7M). Control tracks (Ct) contained no drug.

GCCGC in the 117-mer and 178-mer, respectively, were significantly protected from DNAase I cleavage in the presence of the drug. There was no room for doubt that the binding of the alkaloid to GC sequences was much favored over binding to AT or mixed sequences. The results are directly reminiscent to those reported a few years ago with an ellipticine derivative which also produced a selective effect upon GC-rich sequences (*53*).

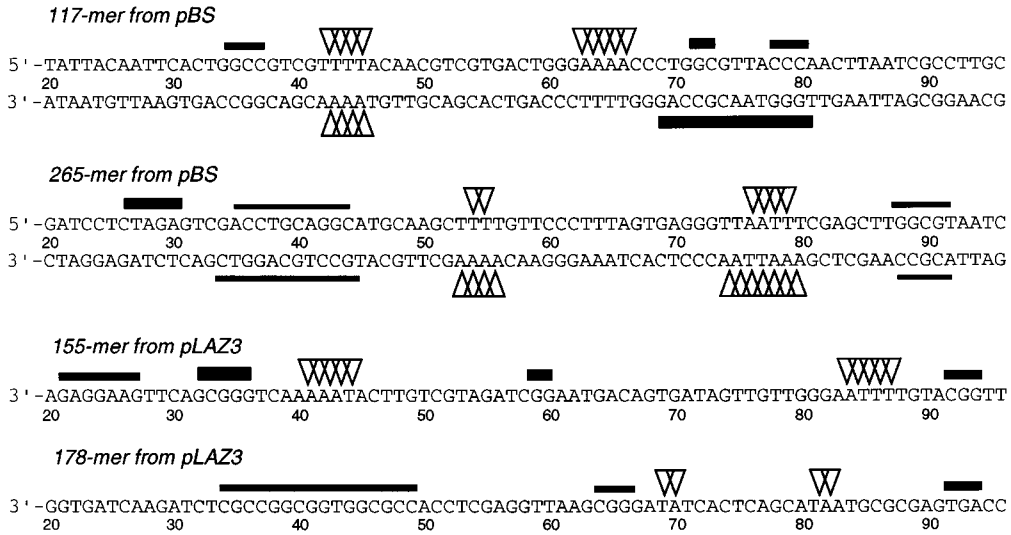

FIGURE 8: Summary map representing the DNAase I footprints detected with cryptolepine on the four DNA fragments studied: the 117 and 265 base-pair fragments from plasmid pBS and the 155 and 178 base-pair fragments from plasmid pLAZ3. Only the region of the restriction fragments analyzed by densitometry is shown. Open arrowheads denote the sites of drug-induced enhanced reactivity toward DNAase I. The black boxes indicate the positions of inhibition of DNAase I cutting in the presence of cryptolepine (presumptive binding sites inferred from differential cleavage plots). Data are compiled from quantitative analysis of three sequencing gels such as the one shown in Figure 7 and must be considered as a set of averaged values.

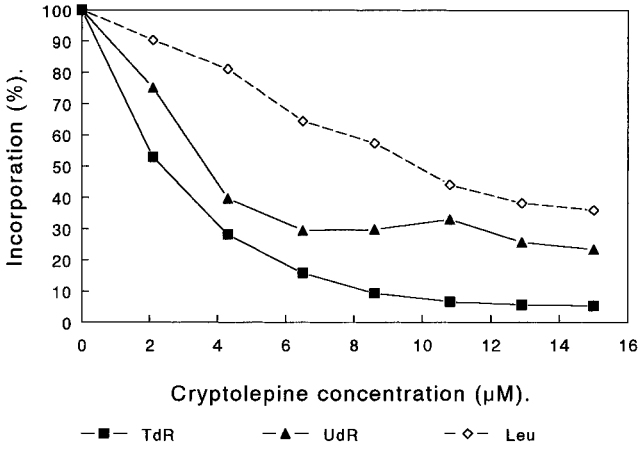

FIGURE 9: Effects of cryptolepine on the biosynthesis of DNA [(^{3}H)TdR], RNA [(^{3}H)UdR] and protein [(^{3}H)Leu] after 4 h of treatment in B16 melanoma cells cultured *in vitro*. Control values (no drug) were considered as 100%.

Effects of Cryptolepine on B16 Melanoma Cells. To test the cytotoxicity of cryptolepine on cancer cells, we decided to perform an *in vitro* cell survival assay using the MTT test. An IC_{50} value of +0.3 μg/mL (1.3 μM) was measured with cryptolepine, whereas under the same conditions (3 days continuous exposure) an IC_{50} of +1.3 μg/mL (5.3 μM) was obtained with ellipticine. Cryptolepine proves to be significantly more toxic to B16 cells than ellipticine.

The effects of cryptolepine on nucleic acids and protein synthesis were then analyzed after 4 h of contact with the drug, at different concentrations, and in the presence of (^{3}H)-Leu, (^{3}H)UdR, or (^{3}H)TdR (Figure 9). Cryptolepine inhibits primarily the DNA synthesis (50% at 0.55 μg/mL, i.e., 2.4 μM). Higher drug concentrations are required to inhibit the synthesis of RNA (50% at 0.85 μg/mL, i.e., 3.7 μM), and proteins (50% at 2.3 μg/mL, i.e., 10 μM). A Feulgen reaction was performed, and the DNA content was measured in individual cells at 580 nm absorbance with the CAS (Cell Analysis Systems) system. We observed a slight increase of cell number in the G_2/M phase of the cell cycle after 20 h (4 and 7%) or 48 h (6 and 9%) treatment with cryptolepine (0.45 and 2.2 μM, respectively) (data not shown). Concomitantly, a weak decrease of cell number in the G_1 phase was noted. At 4.4 μM (1 μg/mL) cryptolepine, the number of cells in the G_2/M phase was doubled after treatment for 20 h and was more than tripled after incubation for 48 h. (Figure 10). The incorporation of cryptolepine on living cells is very fast. Under the fluorescence microscope, the nuclei of cryptolepine-treated cells appeared first brightly fluorescent after a 5 min incubation. A prolonged exposure (15

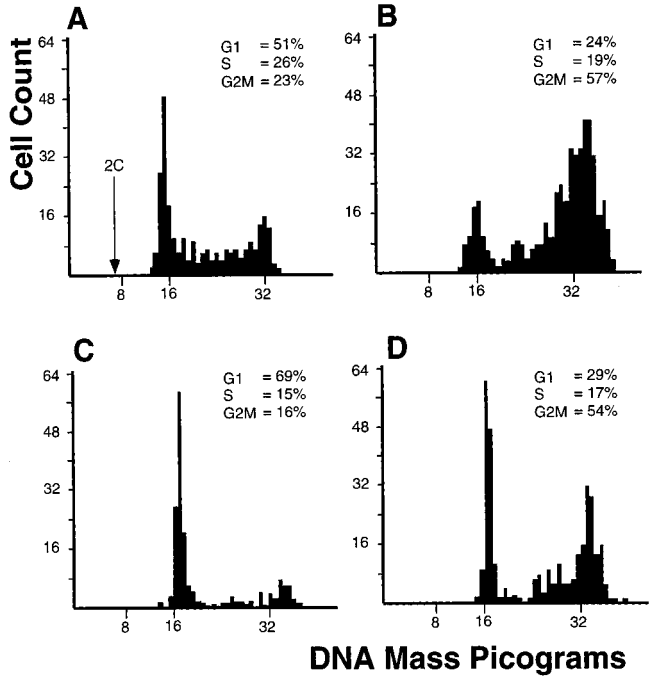

FIGURE 10: Distribution of cells in function of the DNA contents (in picograms) for (A) control after 20 h in culture, (B) cells treated 20 h with cryptolepine 1 μg/mL (4.4 μM), (C) control after 48 h in culture, and (D) cells treated 48 h with cryptolepine 1 μg/mL. The 2*C* value corresponds to the predeposited diploid reference cells. The percentages of B16 cells in the different phases of the cell cycle (G_1, S, and G_2M) are indicated.

min) rendered the entire body of the cells (both the cytoplasm and the nucleus) fluorescent (data not shown). This suggests that the primary target of the drug is localized in the nuclear compartment and is consistent with an effect at the DNA level.

CONCLUSION

The results of the complementary spectroscopic, biochemical, and cellular studies are highly consistent and prove that the genetic material is the primary target of cryptolepine. At the molecular level, the absorption, fluorescence, CD, and ELD measurements reinforced by the topoisomerization data leave no room for doubt that cryptolepine intercalates into DNA. It was not possible to undertake viscosity measurements due to the limited solubility of the drug in aqueous buffer, but all the data concur to indicate that the drug behaves as a typical intercalating agent. This explains our previous observations that cryptolepine competes with the triphenylmethane dye methyl green for binding to DNA (*26*). Furthermore, its displacement activity was as strong as doxorubicin. In many aspects, the results are comparable to those previously obtained with ellipticines which present a structurally related planar chromophore (*22*, *23*). The DNA binding process is tight and geometrically homogeneous. No external or groove binding reaction was detected, and the affinity constant of the drug for double-stranded DNA falls in the range of the values commonly obtained with typical intercalating agents. In addition, the drug exhibits a noticeable preference for GC-rich sequences and affects topoisomerase II activity. The key observation that the alkaloid proves capable of stimulating topoisomerase II-mediated cleavage of DNA may be related to its antitumor activity, as many intercalating antitumor agents (e.g., adriamycin, mitoxantrone, bisantrene, and amsacrine) are topoisomerase II inhibitors.

At the cellular level, it is interesting to note that the drug is more potent at inhibiting the synthesis of DNA rather than RNA and proteins in B16 melanoma cells. Very likely, this accounts for the capacity of the drug (i) to concentrate selectively into the cell nuclei, (ii) to intercalate into DNA, and (iii) to block the cell cycle at the end of the DNA replication phase (late S and G_2/M). Similar effects have been reported with other natural alkaloids including ellipticine. Cryptolepine which is 4−5 times more cytotoxic than ellipticine toward B16 melanoma cells is therefore a valid candidate for the development of tumor-active compounds. The present findings provide encouragement to continue the search for new alkaloids from plants and thereby perhaps the discovery of original molecules active against untreatable solid tumors. The vegetal world is largely untapped as a source of useful drugs.

REFERENCES

1. Clinquart, E. D. (1929) *Bull. Acad. R. Méd. 9*, 627−635.
2. Delvaux, E. (1931) *J. Pharm. Belg. 13*, 955−959.
3. Gellert, E., Raymond-Hamet, and Schlittler, E. (1951) *Helv. Chim. Acta 34*, 642−651.
4. Dwuma-Badu, D., Ayim, S. K., Fiagbe, N. I. Y., Knapp, J. E., Schiff, Jr., P. L., and Slatkin, D. J. (1978) *J. Pharm. Sci. 67*, 433−434.
5. Ablordeppey, S. A., Hufford, C. H., Borne, R. F., and Dwuma-Badu, D. (1990) *Planta Med. 56*, 416−417.
6. Tackie, A. N., Sharaf, M. H. M., Schiff, P. L., Jr., Boye, G. L., Crouch, R. C., and Martin, G. E. (1991) *J. Heterocycl. Chem. 28*, 1429−1435.
7. Gunatilaka, A. A. L., Sotheeswaran, S., Balasubramaniam, S., Chandrasekara, A. I., and Badra Sriyani, H. T. (1980) *Planta Med. 39*, 66−72.
8. Raymond-Hamet (1937) *C. R. Soc. Biol. 126*, 768−770.
9. Raymond-Hamet (1938) *C. R. Acad. Sci. Belg. 207*, 1016−1018.
10. Noamesi, B. K., and Bamgbose, S. O. A. (1980) *Planta Med. 39*, 51−56.
11. Noamesi, B. K., and Bamgbose, S. O. A. (1982) *Planta Med. 44*, 241−245.
12. Rauwald, H. W., Kober, M., Mutschler, E., and Lambrecht, G. (1992) *Planta Med. 58*, 486-488.
13. Bamgbose, S. O. A., and Noamesi, B. K. (1981) *Planta Med. 41*, 392−396.
14. Boakye-Yiadom, K., and Heman-Ackah, S. M. (1979) *J. Pharm. Sci. 68*, 1510−1514.
15. Paulo, A., Pimentel, M., Viegas, S., Pires, I., Duarte, A., Cabrita, J., and Gomes, E. T. (1994) *J. Ethnopharmacol. 44*, 73−77.
16. Paulo, A., Duarte, A., and Gomes, E. T. (1994) *J. Ethnopharmacol. 44*, 127−130.
17. Cimanga, K., De Bruyne, T., Lasure, A., Van Poel, B., Pieters, L., Claeys, M., VandenBerghe, D., Kambu, K., Tona, L., and Vlietinck, A. J. (1996) *Planta Med. 62*, 22−27.
18. Kirby, G. C., Paine, A., Warhurst, D. C., Noamesi, B. K., and Phillipson, J. D. (1995) *Phytother. Res. 9*, 359−363.
19. Grellier, P., Ramiaramanana, L., Millerioux, V., Deharo, E., Schrevel, J., Frappier, F., Trigalo, F., Bodo, B., and Pousset, J. L. (1996) *Phytother. Res. 10*, 317−321.
20. Wright, C. W., Phillipson, J. D., Awe, S. O., Kirby, G. C., Warhurst, D. C., Quetin-Leclercq, J., and Angenot, L. (1996) *Phytother. Res. 10*, 361−363.
21. Cimanga, K., De Bruyne, T., Pieters, L., Vlietinck, A. J., and Turger, C. A. (1997) *J. Nat. Prod. 60*, 688−691.
22. Kohn, K. W., Waring, M. J., Glaubiger, D., and Friedman, C. A. (1975) *Cancer Res. 35*, 71−76.
23. Fossé, P., Paoletti, C., and Saucier, J. M. (1988) *Biochem. Biophys. Res. Commun. 151*, 1233−1240.
24. Le Pecq, J. B., Gosse, C., Dat-Xuong, N. G., Cros, S., and Paoletti, C. (1976) *Cancer Res. 36*, 3067−3076.
25. Artega, C. L., Kisner, D. L., Goodman, A., and Von Hoff, D. D. (1987) *Eur. J. Cancer Clin. Oncol. 23*, 1621−1626.
26. Bonjean, K., De Pauw-Gillet, M. C., Bassleer, R., Quetin-Leclercq, J., Angenot, L., and Wright, C. W. (1996) *Phytother. Res. 10*, S159−S160.
27. Kreuzer, K. N. (1989) *Pharmacol. Ther. 43*, 377−395.
28. Capranico, G., and Zunino, F. (1995) *Curr. Pharm. Des. 1*, 1−14.
29. Wells, R. D., Larson, J. E., Grant, R. C., Shortle, B. E., and Cantor, C. R. (1970) *J. Mol. Biol. 54*, 465−497.
30. Fredericq, E., and Houssier, C. (1973) in *Electric Dichroism and Electric Birefringence*, Clarendon Press, Oxford.
31. Houssier, C., and O'Konski, C. T. (1981) in *Molecular Electrooptics* (Krause, S., Ed.) pp 309−339, Plenum Publishing Corp., New York.
32. Houssier, C. (1981) in *Molecular Electrooptics* (Krause, S., Ed.) pp 363−398, Plenum Publishing Corp., New York.
33. Bailly, C., Hénichart, J.-P., Colson, P., and Houssier, C. (1992) *J. Mol. Recognit. 5*, 155−171.
34. Colson, P., Bailly, C., and Houssier, C. (1996) *Biophys. Chem. 58*, 125−140.
35. Kerckaert, J.-P., Deweindt, C., Tilly, H., Quief, S., Lecocq, G., and Bastard, C. (1993) *Nat. Genet. 5*, 66−70.
36. Bailly, C., and Waring, M. J. (1995) *J. Biomol. Struct. Dyn. 12*, 869−898.
37. Mosmann, T. (1983) *J. Immunol. Methods 65*, 55−63.
38. Bacus, J. W., and Grace, L. J. (1987) *Appl. Opt. 26*, 3280−3293.
39. Taylor, S. R., Titus-Ernstoff, L., and Stitely, S. (1989) *Cytometry 10*, 382−387.

40. Cantor, C. R., and Schimmel, P. R. (1980) *Biophysical Chemistry*, W. H. Freeman and Co., San Francisco.
41. Wilson, W. R., Baguley, B. C., Wakelin, L. P. G., and Waring, M. J. (1981) *Mol. Pharmacol. 20*, 404−414.
42. Houssier, C., Hardy, B., and Fredericq, E. (1974) *Biopolymers 13*, 1141−1160.
43. Fredericq, E., and Houssier, C. (1972) *Biopolymers 11*, 2281−2308.
44. Bourdouxhe, C., Colson, P., Houssier, C., Sun, J. C., Montenay-Garestier, T., Hélène, C., Rivalle, C., Bisagni, E., Waring, M. J., Hénichart, J.-P., and Bailly, C. (1992) *Biochemistry 31*, 12385−12396.
45. Bailly, C., Michaux, C., Colson, P., Houssier, C., Sun, J. S., Garestier, T., Hélène, C., Hénichart, J.-P., Rivalle, C., Bisagni, E., and Waring, M. J. (1994) *Biochemistry 33*, 15348−15364.
46. Nordén, B., and Kurucsev, T. (1994) *J. Mol. Recognit. 7*, 141−156.
47. Bailly, C., O'Huigin, C., Houssin, R., Colson, P., Houssier, C., Rivalle, C., Bisagni, E., Hénichart, J.-P., and Waring, M. J. (1992) *Mol. Pharmacol. 41*, 845−855.
48. Covey, J. M., Kohn, K. W., Kerrigan, D., Tilchen, E. J., and Pommier, Y. (1988) *Cancer Res. 48*, 860−865.
49. Nelson, E. M., Tewey, K. M., and Liu, L. F. (1984) *Proc. Natl. Acad. Sci. U.S.A. 81*, 1361−1365.
50. Rowe, T. C., Chen, G. L., Hsiang, Y. H., and Liu, L. F. (1986) *Cancer Res. 46*, 2021−2026.
51. Tewey, K. M., Chen, G. L., Nelson, E. M., and Liu, L. F. (1984) *J. Biol. Chem. 259*, 9182−9187.
52. Fossé, P., René, B., Saucier, J.-M., Nguyen, C. H., Bisagni, E., and Paoletti, C. (1990) *Biochem. Pharmacol. 39*, 669−676.
53. Bailly, C., O'Huigin, C., Rivalle, C., Bisagni, E., Hénichart, J.-P., and Waring, M. J. (1990) *Nucleic Acids Res. 18*, 6283−6291.
54. Delvaux, E. (1931) *J. Pharm. Belg. 13*, 973−976.

BI972927Q